Optimization of magnetoliposomes for biomedical multi-tasking; potential dual contrast agents and drug delivery vehicles.

C. J. Meledandri and D. F. Brougham*

National Institute for Cellular Biotechnology, School of Chemical Sciences, Dublin City University, Dublin 9, Ireland, carla.meledandri2@mail.dcu.ie, dermot.brougham@dcu.ie

ABSTRACT

Magnetic iron oxide nanoparticles were synthesized and stabilized inside phospholipid vesicles by two different methods. The resulting magnetoliposome suspensions were characterized by dynamic light scattering and NMR. The NMR analysis demonstrated conclusively that the magnetic cores of the magnetoliposomes contained clusters of smaller, superparamagnetic primary particles. The application of magnetic filtration at various flow rates allowed control over the final size of the magnetoliposomes, as well as improved MRI characteristics upon removal of excess phopsholipids from the aqueous suspensions. In all cases the liposome size distribution, with mean values from 70-150 nm, was unchanged over 80 days.

Keywords: magnetoliposomes, contrast agents, drug delivery, MRI, NMR

1 INTRODUCTION

Magnetoliposomes, liposomes which incorporate magnetic nanoparticles, are of interest due to their low toxicity and potential applications as contrast agents for MRI and as drug delivery vehicles. These applications are strongly dependent on control of the overall particle size, on the nature of the primary particle (superparamagnetic or multi-domain) and on the iron loading. There has been significant focus on control of the synthetic conditions [1] and also on magnetic filtration of the resulting suspensions [2]. In aqueous suspension magnetic nanoparticles (NPs) produce strong magnetic resonance relaxation enhancements. This effect is quantified as the concentration independent spin-lattice, or spin-spin relaxivity (r_1 and r_2, respectively), i.e. the relaxation rate enhancement per mmole of iron. For magnetite suspensions r_1 and r_2 range from 10-30 and 100-200 $s^{-1}mM^{-1}$, respectively, in the clinical MRI field range of 40-120 MHz. [3]

Magnetic particles stabilized in suspension with phospholipids (PLs) were first described by de Cuyper et al. [4]. Preparation involved the incubation and dialysis of surfactant stabilized magnetic particles with preformed PL vesicles to produce magnetoliposomes (MLs). In this 'solid'-type ML, the interior of the lipid vesicle is entirely packed with magnetic material, and inner PL layer is thought to be adsorbed onto the NP surface. Alternatively, a second type of ML has been described [5] in which NPs are encapsulated within the aqueous core of the liposome, prepared by hydrating a lipid film with magnetic fluid. Lesieur et al. [6] have recently demonstrated the advantages of these 'aqueous'-type MLs, with hydrodynamic size in the 195 ± 33 nm range, for MRI imaging. The main drawback of this technique is that it produces relatively large particles which may only find application in gastro-intestinal imaging. Materials that are successfully used parenterally must have extended blood circulation half-lives, which usually requires diameters < 100 nm, and often grafting with polyethylene glycol to avoid rapid recognition by the reticulo-endothelial system.

In this work 'solid' and 'aqueous'-type ML suspensions were prepared, magnetically filtered and characterized by NMR relaxation time measurements and by dynamic light scattering. This paper demonstrates both the utility of magnetic filtration and the morphological differences between 'aqueous' and 'solid'-type magnetolioposmes.

2 EXPERIMENTAL

2.1 Materials

1,2-Dioleoyl-sn-Glycero-3-[Phospho-rac-(1-glycerol)] (Sodium Salt) (DOPG) was purchased as a lyophilized powder (>99%) from Avanti Polar Lipids (Alabaster, AL, USA) and stored at -20°C. Iron (II) chloride tetrahydrate (>99%) was purchased from Fluka (Buchs, Switzerland). Iron (III) chloride-6-hydrate (>99%) was purchased from Riedel-de-Haën (Seelze, Germany). All other chemicals were obtained from Sigma Aldrich (St. Louis, MO, USA) (purity > 99.9%), and all reagents were used without further purification. De-ionised water was de-aerated prior to use.

2.2 Magnetic nanoparticles

Aqueous dispersions of uncoated NPs were prepared by ammonia coprecipitation of iron salts (2:1 molar ratio Fe^{3+}:Fe^{2+}) at 80°C [7]. Upon cooling, the magnetite was precipitated and washed twice with 50:50 MeOH/acetone and isolated between each wash by magnetic decantation. A stable aqueous suspension of uncoated magnetite NPs was obtained following 2-3 washes with H_2O.

Magnetite NPs coated with a monolayer of DOPG were prepared as described above with the following modifications: (i) 13.6 mg DOPG in MeOH was added

immediately before NH_3 addition; (ii) 54.4 mg DOPG in MeOH was slowly added to the suspension immediately after NH_3 addition; (iii) 5 washes with 50:50 MeOH/acetone were performed and the magnetite was isolated by magnetic decantation. Half of the sample was dispersed in $CHCl_3$ for characterization, and the other half was resuspended in H_2O.

2.3 Magnetoliposomes

Magnetoliposomes were prepared by two methods. In the thin film-hydration method, [8] multilamellar MLs were formed by room temperature hydration of a thin film of DOPG with the aqueous suspension of uncoated magnetite, with periodic vortex mixing. The MLs were subjected to freeze-thaw cycles with liquid N_2 to form unilamellar 'aqueous'-type MLs. Samples were then either extruded through polycarbonate membranes with a 0.2 μm pore size (Whatman Nuclepore; Clifton, NJ) using an Avanti Polar Lipids mini extruder (Alabaster, AL), or magnetically filtered. To produce 'solid'-type MLs ammoniated DOPG was added with stirring to monolayer coated NPs redispersed in H_2O at 65°C. Upon cooling, the resulting aqueous suspension was sonicated, then placed over a bar magnet. The supernatant was retained for characterization.

2.4 Magnetic filtration

A variable flow peristaltic pump was used to pump aqueous ML suspensions through 1/8 inch ID tubing packed with ~60 mg of steel wool, which was placed between the poles of a 0.47 T permanent magnet. Flow rates were varied between 4-600 mL/hr. Both the eluent and the retentate were collected for characterization.

2.5 Characterization

Dynamic light scattering experiments were performed at 25°C on a High Performance Particle Sizer HPPS (Malvern Instruments, Malvern, UK) which uses detection angle of 173°, and a 3 mW He-Ne laser at a wavelength of 633 nm. The z-average (mean hydrodynamic) diameter and the polydispersity index (an estimate of the distribution width) were calculated using cumulants analysis.

The water ^1H spin lattice relaxation rates were measured as a function of magnetic field [9] using a Stelar Spinmaster, Fast Field Cycling Relaxometer, (Stelar SRL, Mede, Italy).

Attenuated total reflectance (ATR) infrared spectra were recorded on a Spectrum GX FT-IR System (Perkin Elmer; Norwalk, CT, USA). Liquid samples were placed on the face of a ZnSe trough plate crystal and the solvent was evaporated under N_2. Eight scans were recorded over a 4000-650 cm^{-1} spectral range with 2 cm^{-1} spatial resolution. ATR and baseline corrections were applied followed by 19-point smoothing (Spectum software v.3.01; Perkin Elmer LLC; Norwalk, CT, USA).

Total iron content was determined by atomic absorption spectroscopy on a Varian SpectrAA Spectrometer. The light source was a Fe-cathode lamp with a wavelength of 248.3 nm. ML suspensions were mixed with an equal volume of 5% (v/v) Triton X-100 solution, and the iron oxide cores were then digested with 6N analar grade HCl.

3 RESULTS AND DISCUSSION

3.1 Infrared Spectroscopy

ATR-IR spectra of uncoated magnetite nanoparticles and DOPG coated samples are shown in Fig. 1.

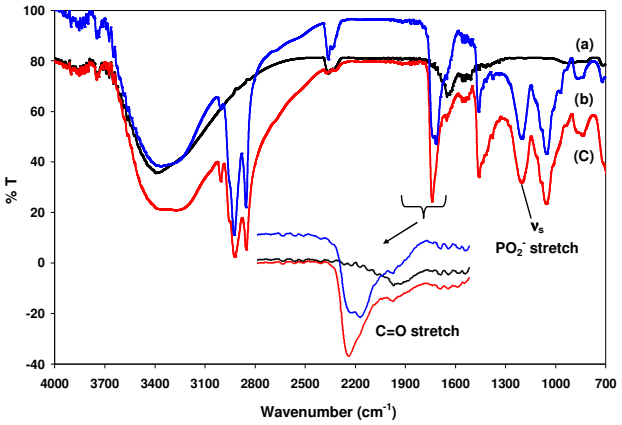

Figure 1: ATR-FTIR spectra of (a) uncoated magnetite NPs (b) 'aqueous' DOPG MLs, (c) 'solid' DOPG MLs.

The infrared spectrum of the bilayer coated magnetite shows several strong absorption bands due to the presence of DOPG. The bands can be assigned as follows: 2922 cm^{-1} and 2853 cm^{-1} are due to asymmetric (ν_a) and symmetric (ν_s) methylene C-H stretch, respectively; 1459 cm^{-1} is caused by ν_s (C-H) scissors mode; the broad band centered around 3237 cm^{-1} is due stretching vibrations of hydrogen bonded and non-hydrogen bonded OH groups; ν_a and ν_s phosphate stretching modes are observed at 1204 cm^{-1} and 1057 cm^{-1}, respectively; the band at 1739 cm^{-1} can be assigned to the two ester carbonyls.

Thus the presence of characteristic PL bands in the IR spectrum of MLs indicated the successful coating of NPs with DOPG. The PL bands were present in the spectra of MLs prepared by both methods. The carbonyl stretching region of the 'aqueous' MLs shows splitting, ascribed to hydrogen bonding to water [10], not observed for the 'solid' type MLs. A 3 cm^{-1} decrease in the frequency of the ν_s phosphate stretch is also observed. Thus the IR suggests that PL is not physisorbed onto magnetite in the case of the 'aqueous'-type ML dispersions.

3.2 NMR relaxometry

The magnetic field dependence of the relaxivity in the ^1H resonance frequency range 0.01-20 MHz, was measured

NSTI-Nanotech 2007, www.nsti.org, ISBN 1420061836 Vol. 2, 2007

using the technique of nuclear magnetic resonance dispersion, NMRD. The NMRD profiles obtained are commonly used to investigate the magnetic properties of the NP dispersions, which determine the MRI response. [3] The generally accepted theory for relaxation of water due to the presence of dispersed superparamagnetic NPs in suspension was developed by Muller and co-workers [3]. The theory extends the classical outer-sphere theory of relaxation to include the presence of a high Curie component, even at moderate fields, and the presence of strong magneto-crystalline anisotropy. The high field relaxation is driven by diffusion of water, with the position of the r_1 maximum sensitive to the primary particle size as it is determined by the characteristic diffusion time, $\tau_D = d^2/(4D)$, where d is the particle diameter and D is the diffusion coefficient. The low-field relaxation is due to fluctuations in the particles moment, i.e. to the Néel process. Using physically acceptable values for the critical parameters; the particle size, Néel correlation time τ_N, saturation magnetization M_s and magnetic anisotropy energy ΔE_{anis}, the theory produces quantitative agreement [3] with the measured profiles of suspensions of superparamagnetic particles.

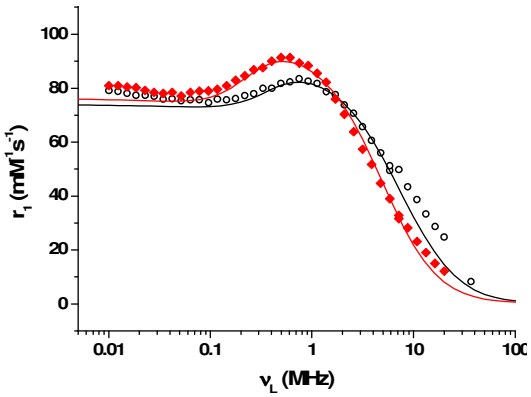

Figure 2: NMRD profiles, at 295K, of 'solid' type MLs (○) and 'aqueous' type (♦). Solid lines are the simulated profiles using Muller's cluster model [3].

Relaxivity profiles, Fig 2, for aqueous suspensions of magnetoliposomes, prepared by either method, do not conform to this model as it predicts a low-field plateau at r_1 ~10-20 $s^{-1}mM^{-1}$ for 10 nm particles. Included in this figure are simulated profiles using an extension of Muller's model developed for clustered superparamagnetic crystals within a permeable coating. [3] This model assumes that relaxation of water by diffusion into the magnetic cluster is analogous to a chemical-exchange problem.

The reasonable fits to the experimental data suggests that the MLs prepared by both methods contain larger clusters composed of superparamagnetic primary particles. Most of the fitting parameters used to fit the two profiles were similar; the radius of the superparamagnetic primary nanoparticles was 9-10 nm, M_s = 36 emu/g, τ_N = 60 ns, ΔE_{anis} = 5 GHz. For the 'solid'-type (○) preparation the magnetic cluster diameter obtained from NMR was 96 nm, which compares well with the Z-avg diameter of 90 nm. For the 'aqueous'-type preparation (♦), the magnetic cluster diameter obtained was 62 nm, while the mean hydrodynamic diameter was 128 nm. This result is consistent with the expected liposome morphology from the two types of preparation. For the 'solid' preparation the magnetic clusters are stabilized by lipid and dispersed in water and the cluster sizes obtained from NMR and light scattering are similar; for the 'aqueous' preparations the magnetic clusters are further encapsulated in an aqueous compartment and the hydrodynamic size is larger than that of the cluster. It is likely therefore that the aqueous method of preparation could produce magnetically targeted delivery vehicles which are suitable for hydrophilic drugs.

3.3 Magnetic filtration

The average hydrodynamic diameter (Z-Avg) and polydispersity index (PDI) of magnetically filtered 'solid'-type ML suspensions are reported in Table 1 as a function of flow rate. The intensity distributions of two magnetically filtered samples with Z-Avg ±40 nm are shown below in Fig. 3.

	Eluent		Retentate	
Flow Rate (mL/hr)	**Z-Avg (nm)**	**PDI**	**Z-Avg (nm)**	**PDI**
4	*	*	94.5	0.201
105	70.4	0.210	106	0.222
210	71.2	0.177	111	0.196
315	74.9	0.174	110	0.224
600	78.9	0.171	111	0.260

Table 1: The effect of magnetic filtration and sample flow rate on the Z-Avg and PDI of 'solid' MLs dispersed in both the eluent and the retentate. Original sample: Z-Avg=90.4 nm, PDI=0.195. *At this flow rate the eluent was non-magnetic, consisting of PLs only.

Regardless of the preparation method, the unprocessed ML suspensions undoubtedly contain excess PL molecules. The application of magnetic fields was used to separate the excess PLs from the MLs, and this resulted in an increase in the relaxation rate of the ML samples (data not shown). In addition to PL removal our results show that by adjusting the rate at which the ML suspensions were pumped through the magnetic filtration system, we could exert control over the final average particle size of the samples. At the slowest flow rates, for most particles the magnetic force from the external magnetic field (proportional to particle diameter) exceed the weaker force of the flow, and therefore only the smallest particles were collected in the eluent and the larger MLs were retained on the steel wool. As the flow rate was increased, larger particles appeared in the eluent. As the smaller particles were eliminated from the bulk sample, the average size of the particles suspended in the retentate was found to increase. Magnetic filtration at a flow rate of 210

mL/hr allowed a division of the bulk sample into two fractions (eluent, retentate) which differed in mean particle size by 40 nm, while the polydispersity of the suspensions were similar, Fig. 3.

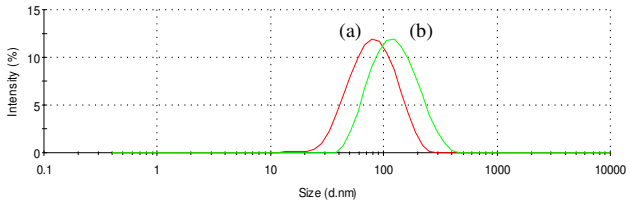

Figure 3: PCS size distributions of 'solid' type MLs dispersed in water following magnetic filtration at a flow rate of 210 mL/hr; (a) the eluent, Z-Avg = 71.2 nm, PDI=0.177, (b) the retentate, 111 nm (0.196).

The size selection capability of magnetic filtration has great potential for use in the production of homogenous 'aqueous'-type MLs of a specific size by the hydration-freeze thaw method. Currently, extrusion is a widely accepted, reproducible means of producing homogenous liposome suspensions with a unimodal particle size distribution [11], but this technique has limitations; sample concentration, volume, and liposome size, which is limited by the pore sizes of the membranes commercially available. These limitations do not apply to magnetic filtration, thus making it a possible alternative to extrusion. Furthermore, as MLs are retained as solid particles on the magnetic steel wool during the filtration procedure, varying the volume of water used to redisperse and collect the particles allows control of the final sample concentration.

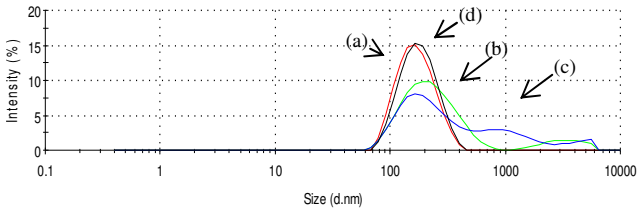

Figure 4: Intensity size distributions at each stage of the 'aqueous' ML preparation (a) uncoated magnetite; Z-Avg = 157 nm, PDI = 0.146; (b) hydration only, 200 nm (0.354); (c) hydration + freeze-thaw, 239 nm (0.442); (d) hydration + freeze-thaw + magnetic filtration, 164 nm (0.112).

Figure 4 shows the intensity size distributions at each stage of an 'aqueous'-type ML preparation utilizing magnetic filtration as opposed to extrusion. Extrusion at 200 nm resulted in an average ML diameter of 148 nm and a PDI of 0.194 (results not shown), while magnetic filtration at an optimal flow rate resulted in an average diameter of 164 nm with a much improved PDI of 0.112. PCS confirmed that the ML samples, prepared by both methods, were stable. The hydrodynamic diameters were unchanged after 80 days and most had slightly better polydispersity.

4 CONCLUSIONS

Our ongoing research is to optimize ML preparations, to produce suspensions of particles smaller than 100 nm. We have found that magnetic filtration can be used to remove non-magnetic material and also for selective particle size control. Magnetic separation has many potential advantages; it is a fast, efficient, and inexpensive method that can be used for suspensions of any concentration and it can be easily scaled up. We have also found significant differences in the physical characteristics of 'solid' and 'aqueous' types of ML dispersions. Future work will include cryo-TEM investigations into these different types of suspension.

5 ACKNOWLEDGEMENTS

CM is supported by the National Institute for Cellular Biotechnology, and by an Enterprise Ireland Proof of Concept Award (PC/2006/207). DB acknowledges the Higher Education Authority of the Republic of Ireland for support in equipment purchase.

REFERENCES

[1] S. Sun and H. Zeng, J. Am. Chem. Soc., 124, 8204-8205, 2002.

[2] C. T. Yavus, J. T. Mayo, W. W. Yu, A. Prakash, J. C. Falkner, S. Yean, L. Cong, H. J. Shipley, A. Kan, M. Tomson, D. Natelson and V. L. Colvin, Science, 314, 964-967, 2006.

[3] (a) R. N. Muller, A. Roch, J.-M. Colet, A. Ouakssim and P. Gillis, "The Chemistry of Contrast Agents in Medical Magnetic Resonance Imaging", A. E. Merbach, E. Toth (Eds), John Wiley and Sons, 417-435, 2001. (b) A. Roch, Y. Gossuin, R. N. Muller and P. Gillis, J. Magn. Magn. Mater., 293, 532-539, 2005. (c) A. Roch, R. N. Muller, P. Gillis, J. Chem. Phys., 110, 5403-5411, 1999.

[4] M. De Cuyper and M. Joniau, Eur. Biophys. J., 15, 311-319, 1988.

[5] M.-S. Martina, J.-P. Fortin, C. Ménager, O. Clément, G. Barratt, C. Grabielle-Madelmont, F. Gazeau, V. Cabuil and S. Lesieur, J. Am. Chem. Soc., 127, 10676-10685, 2005.

[6] S. Lesieur, C. Grabielle-Madelmont, C. Menager, V. Cabuil, D. Dadhi, P. Pierrot and K. Edwards, J. Am. Chem. Soc., 125, 5266-5267, 2003.

[7] S. E. Khalafalla and G. W. Reimers, IEEE Trans. Magn. 16, 178-183, 1980.

[8] D. D. Lasic, "Liposomes: From Physics to Applications," Elsevier, 1993.

[9] R. Kimmich and E. Anoardo, Prog. Nuc. Magn. Reson. Spec., 44, 257-320, 2004.

[10] A. Nilsson, A. Holmgren, A and G. Lindblom, Biochemistry, 30, 2126-2133, 1991.

[11] F. Szoka Jr. and D. Papahadjopoulos, Ann. Rev. Biophys. Bioeng., 9, 467-508, 1980.